ACS OMEGA

http://pubs.acs.org/journal/acsodf

Article

Significantly Enhanced Thermal Decomposition of Mechanically Activated Ammonium Perchlorate Coupling with Nano Copper Chromite

Dongdong Zhang, Qiang Li, Ruiqin Li, Hao Li, Hongxu Gao, Fengqi Zhao, Lei Xiao,* Guangpu Zhang,* Gazi Hao, and Wei Jiang

Cite This: *ACS Omega* 2021, 6, 16110−16118

Read Online

ACCESS | Metrics & More | Article Recommendations

ABSTRACT: In this article, nano-$CuCr_2O_4$ (copper chromite)/ultrafine ammonium perchlorate (AP) composites were prepared by a ultrasonic dispersion method and a mechanical grinding method. A series of nano-$CuCr_2O_4$/ultrafine AP composites with different dispersions were prepared by controlling the compounding time to study the best catalytic effect of nano-$CuCr_2O_4$ on the ultrafine AP. The microstructures, surface elements, and morphologies of samples were analyzed by X-ray diffraction, Fourier transform infrared spectroscopy, scanning electron microscopy, and energy dispersion X-ray spectroscopy. The catalytic effect of nano-$CuCr_2O_4$ on the thermal decomposition of AP was investigated by differential scanning calorimetric techniques and thermogravimetric analysis. The results indicated that the mechanical ball milling method could make nano-$CuCr_2O_4$ more evenly dispersed on the ultrafine AP, and with the increase in the milling time, the uniformity of nano-$CuCr_2O_4$ on the ultrafine AP was better. When the milling time was 6−12 h, nano-$CuCr_2O_4$ was most evenly dispersed on the ultrafine AP. At this time, the decomposition temperature and Gibbs free energy of the nano-$CuCr_2O_4$/ultrafine AP composite were the lowest, which decreased by 78.1 °C and 25.16 kJ/mol compared with those of ultrafine AP, respectively. Moreover, the mechanical sensitivity of nano-$CuCr_2O_4$/ultrafine AP composites was lower than that of ultrafine AP. It showed that ball milling for 6−12 h could make nano-$CuCr_2O_4$ evenly dispersed on the ultrafine AP, and nano-$CuCr_2O_4$ could play the best catalytic effect on the ultrafine AP.

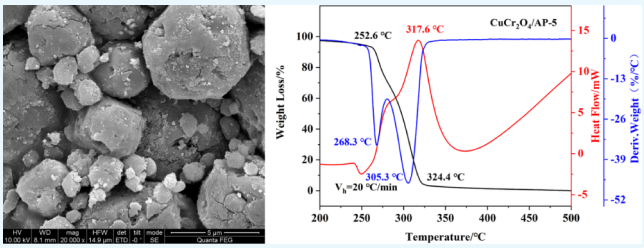

1. INTRODUCTION

Ammonium perchlorate (AP) is the most widely used oxidant in the propellant applications, and its content in propellant accounts for a large proportion, usually exceeding 60%.[1,2] As a strong oxidant, the thermal decomposition of AP provides the oxygen needed for the combustion of the propellant and releases a large amount of energy during the decomposition process to promote the combustion of the propellant.[3,4] Therefore, the pyrolysis of AP plays a decisive role in the combustion performance of the propellant.[5] To be specific, decreasing decomposition temperatures of the AP decomposition process will lead to shorter ignition delay time and higher burning rate of the propellant.[6]

A lot of studies have shown that the burning rate of propellant can be increased by decreasing the particle diameter of AP[7−9] as well as employing some combustion catalyst to AP.[10,11] For example, Dolgoborodov et al. used a planetary ball mill method to prepare ultrafine AP of size 5−10 μm, and the temperature of the ultrafine AP thermal decomposition decreased by more than 100 °C than raw AP with a particle size of 1000 μm.[12] Compared with the reduction in the particle size of AP, the addition of combustion catalysts to AP has caught most attention. Among these catalysts, copper chromite, a mixed oxide of CuO and Cr_2O_3, is well-known burn rate modifier for combustion of propellants, which can accelerate the thermal decomposition of AP and increase the burn rate of propellant combustion. Especially when the catalyst reaches the nanometer size, it can better exert its catalytic effect. For example, Sanoop et al. prepared copper chromite nanoparticles by the thermal decomposition of basic copper ethylamine chromate to catalyze AP decomposition and decreased AP decomposition temperature from 378.5 to 338.6 °C.[13] Hosseini et al. synthesized copper chromite spinel nanoparticles ($CuCr_2O_4$ SNPs) via the sol−gel route and studied its catalytic effect on AP in $CuCr_2O_4$ SNPs/AP composite prepared by the solvent/nonsolvent route. The

Received: April 14, 2021
Accepted: June 3, 2021
Published: June 10, 2021

Table 1. Prepration of a Series of Nano-$CuCr_2O_4$/Ultrafine AP Composites with Different Dispersions

number of samples	1	2	3	4	5	6	7	8
nano-$CuCr_2O_4$/ultrafine AP composites	ultrasonic for 30 min	ball milling for 30 min	ball milling for 1 h	ball milling for 3 h	ball milling for 6 h	ball milling for 12 h	ball milling for 24 h	ball milling for 48 h

results showed that the addition of $CuCr_2O_4$ SNPs to AP remarkably decreased the decomposition temperature from 422.5 °C for pure AP to 338.6 °C for AP containing $CuCr_2O_4$ SNP additive with a mass ratio of 5% and improved the heat released from 879.5 J/g for pure AP to 1474.5 J/g for $CuCr_2O_4$ SNPs/AP composite.[14] Further research found that uniformly compounding the nanocatalyst and AP can further enhance its catalytic effect on AP. Eslami et al. fabricated the AP/$CuCr_2O_4$ core−shell nanocomposites containing $CuCr_2O_4$ additive with a mass ratio of 6% by a feasible deposition method and found that the decomposition temperature of AP composites was at 346 °C, which decreased by 74 °C compared to AP, and the apparent decomposition heat of AP composite was about three times that of AP, changing from 450 J/g for AP to 1510 J/g for AP composite.[15]

Currently, little attention has been paid to the catalysis of ultrafine AP. In fact, evenly compounding the nanocatalyst with the ultrafine AP can significantly improve the thermal decomposition performance of the AP.[16,17] Therefore, nano-$CuCr_2O_4$/ultrafine AP composites would be prepared by an ultrasonic dispersion method and a mechanical grinding method, and the best catalytic effect of nano-$CuCr_2O_4$ on ultrafine AP was studied in this work.

2. EXPERIMENT

2.1. Materials. All the reagents were of analytical grade except AP and directly used without further purification. AP was of industrial grade and was purchased from Dalian Perchloric Acid Ammonium Factory. $CuCr_2O_4$ was purchased from Sinopharm Chemical Reagent Co., Ltd. Ethyl acetate was purchased from Nanjing Chemical Reagent Co., Ltd. Nano-$CuCr_2O_4$ with an average diameter of 50 nm was prepared by mechanical grinding. Ultrafine AP was prepared by air flow crushing method and its particle was 1−5 μm.

2.2. Preparation of Nano-$CuCr_2O_4$/Ultrafine AP Composites. The nano-$CuCr_2O_4$/ultrafine AP composites were prepared by ultrasonic dispersion and mechanical ball milling methods. First, nano-$CuCr_2O_4$/ultrafine AP composite was prepared by the ultrasonic dispersion method. The nano-$CuCr_2O_4$ and ultrafine AP were mixed at a molar ratio of 3:97 to form a mixture of 10 g, and the mixture was added to the beaker. Ethyl acetate (5 mL) was added to the beaker, and the amount of ethyl acetate added just covered the mixture powder. The ultrasonic cleaner was turned on, and the nano-$CuCr_2O_4$ and ultrafine AP were compounded by ultrasonic action. After 30 min, the ultrasonic cleaner was turned off. After ultrasonic treatment, the sample was poured into the surface dish and then dried in a 45 °C water bath oven. Nano-$CuCr_2O_4$/ultrafine AP composite was obtained after complete drying.

Then, a series of nano-$CuCr_2O_4$/ultrafine AP composites with different dispersions were prepared by the mechanical ball milling method. The nano-$CuCr_2O_4$ and ultrafine AP were mixed at a molar ratio of 3:97 to form a mixture of 20 g. The mixture was put into 200 mL of ethyl acetate, and the mass concentration of the mixture in the slurry was kept strictly at 8−10%. The slurry was ground and crushed in nanometer pulverizer. The speed of rotation was 1000 rpm. The outlet temperature of slurry was controlled in the range of 15 °C by the chiller. To explore the best catalytic effect of nano-$CuCr_2O_4$ on ultrafine AP, the ball milling time would be controlled. Here, a series of nano-$CuCr_2O_4$/ultrafine AP composites with different dispersions would be prepared by selecting different ball milling times (30 min and 1, 3, 6, 12, 24, and 48 h). After grinding, a slurry of nano-$CuCr_2O_4$/ultrafine AP composites was obtained. The slurry supernatant was removed by siphoning after natural sedimentation of the slurry. The slurry was poured into the surface dish and then dried in a 45 °C water bath oven. Nano-$CuCr_2O_4$/ultrafine AP composites were obtained after complete drying.

Finally, nano-$CuCr_2O_4$/ultrafine AP composites with different dispersions were numbered, and their types and numbers are shown in Table 1. To facilitate the description of different samples in this paper, the samples were named as $CuCr_2O_4$/AP-1, $CuCr_2O_4$/AP-2, $CuCr_2O_4$/AP-3, $CuCr_2O_4$/AP-4, $CuCr_2O_4$/AP-5, $CuCr_2O_4$/AP-6, $CuCr_2O_4$/AP-7, and $CuCr_2O_4$/AP-8.

2.3. Measurements and Characterizations. Powder X-ray diffraction (XRD) patterns were performed with a Bruker Advance D8 instrument equipped with Cu Kα radiation. Fourier transform infrared (FTIR) analysis of the samples was carried out (Nicolet iS10) in the range of 4000−500 cm^{-1}. The morphology of nano-$CuCr_2O_4$/ultrafine AP composites was examined by an S-4800II cold field scanning electron microscopy (Hitachi Corporation, Japan) equipped with an energy dispersion X-ray spectrometer (EDS), and their chemical compositions were determined by EDS.

The thermogravimetric tests were carried out employing an SDT Q600 thermal analyzer with a gas flow rate of 20 mL/min in nitrogen. The selected heating rates were 5, 10, 15, and 20 °C/min. The program temperature was increased from room temperature to about 520 °C at the end. The kinetic parameters for the exothermic decomposition of AP and AP composites with different nanocatalysts were obtained by the Kissinger method.[18]

The sensitivity test in this paper is impact sensitivity test. The impact sensitivity of the samples is determined according to the method 601.2 in GJB 772A-1997. The dosage of the samples used is 50 mg, and the weight of a drop hammer is 5 kg. The test samples are divided into 25 times as a group, and the "lifting method" is used to measure the characteristic drop height of the samples. If there is no explosion, the height of the drop hammer will be increased, and if there is explosion, the height of the drop hammer will be reduced. The range of height is within six grades. For the measured data, use eq 1 to calculate the characteristic drop height

$$\lg H_{50} = Y_0 + d(A/n \pm 0.5) \quad (1)$$

$$A = \sum in_i$$

where n is the total number of experiments; d is the logarithm of step size; Y_0 is the logarithm of the characteristic height when the stimulus number is "0"; i is the stimulus number, and its values are i= ±1, ±2, and so on. If the value is smaller than

https://doi.org/10.1021/acsomega.1c02002
ACS Omega 2021, 6, 16110−16118

Y_0, it is negative, and if it is larger, it is positive; and n_i is the number of explosions when the stimulus number is i.

3. RESULTS AND DISCUSSION

3.1. XRD and FTIR Analysis. The structural information of nano-$CuCr_2O_4$/ultrafine AP composites is analyzed using XRD and FTIR. Figure 1 shows the XRD pattern of ultrafine AP and nano-$CuCr_2O_4$/ultrafine AP composites, respectively. It can be seen from Figure 1 that the characteristic diffraction peaks of nano-$CuCr_2O_4$/ultrafine AP composites with different dispersions are basically the same, only the intensity of the diffraction peaks is different. According to the XRD pattern of $CuCr_2O_4$/AP-1, the characteristic diffraction peaks of its XRD pattern are completely consistent with those of the ultrafine AP. It shows that in the process of preparing nano-$CuCr_2O_4$/ultrafine AP composites, the ultrafine AP does not participate in the reaction, and the crystal form of ultrafine AP does not change, only physical and mechanical composites occur. However, the characteristic peaks of nano-$CuCr_2O_4$ are not found in the XRD spectrum of nano-$CuCr_2O_4$/ultrafine AP composites, which are mainly because the intensity of the characteristic diffraction peaks of ultrafine AP is too large, and the content of nano-$CuCr_2O_4$ is too small to reach the detection range.[19] Therefore, the XRD pattern of nano-$CuCr_2O_4$ is not listed in the figure to compare with that of $CuCr_2O_4$/AP-1.

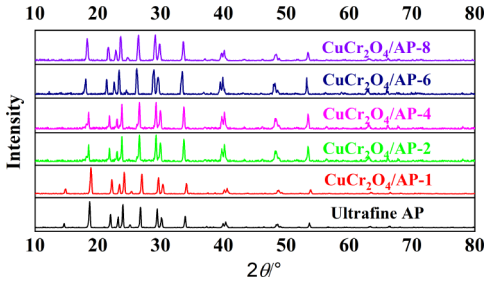

Figure 1. XRD patterns of ultrafine AP and nano-$CuCr_2O_4$/ultrafine AP composites.

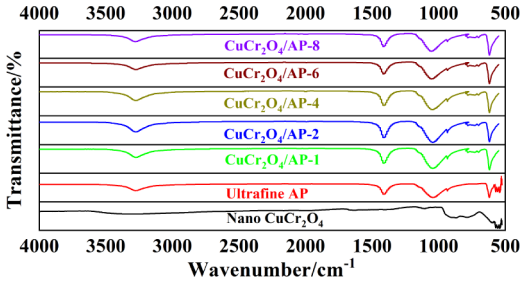

Figure 2. FTIR spectrums of ultrafine AP, nano-$CuCr_2O_4$, and nano-$CuCr_2O_4$/ultrafine AP composites.

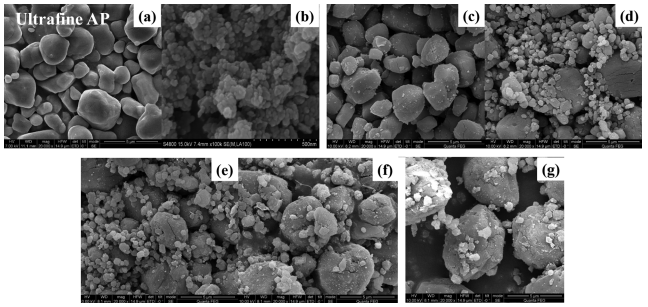

Figure 3. SEM images of (a) ultrafine AP; (b) nano-$CuCr_2O_4$; and nano-$CuCr_2O_4$/ultrafine AP composites: (c) $CuCr_2O_4$/AP-1, (d) $CuCr_2O_4$/AP-2, (e) $CuCr_2O_4$/AP-4, (f) $CuCr_2O_4$/AP-6, and (g) $CuCr_2O_4$/AP-8.

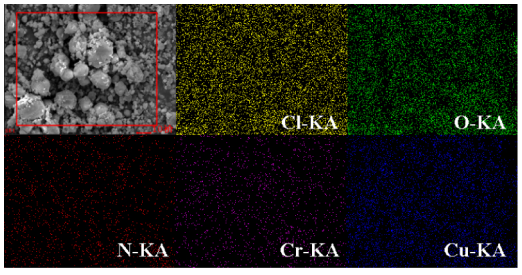

Figure 4. EDS mappings of $CuCr_2O_4$/AP-5.

IR spectrums of nano-$CuCr_2O_4$, ultrafine AP, and nano-$CuCr_2O_4$/ultrafine AP composites are shown in the Figure 2. As shown from the IR spectrum of nano-$CuCr_2O_4$, the observed IR band in the range of 600−540 cm^{-1} can be attributed to a stretching vibration of Cr−O bands of chromium atoms in the tetragonal environment of the O atom.[20] The characteristic peaks of the nano-$CuCr_2O_4$ sample at 691 and 515 cm^{-1} could be attributed to the presence of $Cr_2O_4^{2-}$ group, and the characteristic peak at 884 cm^{-1} refers to Cr−O chromate group.[13,21] For FTIR spectrum of ultrafine AP, the broad absorption bands at 3278 and 1408 cm^{-1} correspond to the N−H stretching vibration and the N−H bending vibration of the AP crystal, respectively. The absorption peak at about 1050 and 622 cm^{-1} correspond to the Cl−O vibration and ClO_4^- vibration absorption, respectively. It can be seen from Figure 2 that the shape and position of the infrared absorption peaks of different nano-$CuCr_2O_4$/ultrafine AP composites are basically the same, so $CuCr_2O_4$/AP-1 is taken as the representative for the analysis. According to the FTIR spectrum of $CuCr_2O_4$/AP-1, there are four obvious infrared absorption peaks, which are consistent with the infrared absorption peaks of ultrafine AP. The stretching vibration absorption peaks of NH_4^+ are around 3277 and 1409 cm^{-1}, and the stretching vibration absorption peaks of ClO_4^- are around 1037 and 615 cm^{-1}.[19] In addition, compared with the ultrafine AP, a new infrared absorption peak appears near 780 cm^{-1}. Compared with the FTIR image of nano-$CuCr_2O_4$, the new infrared absorption peak is the stretching vibration absorption peak of chromate group ($Cr_2O_4^{2-}$), indicating that nano-$CuCr_2O_4$ is compounded on the surface of the ultrafine AP.[15] Through FTIR spectrum, it can be confirmed that nano-$CuCr_2O_4$/ultrafine AP composites can be successfully prepared by the ultrasonic dispersion and mechanical ball milling methods, and in the preparation process, the ultrafine AP does not participate in the reaction, and the crystal form does not change, only physical and mechanical composites occur.

3.2. SEM and EDS Analysis. The morphologies of ultrafine AP, nano-$CuCr_2O_4$, and nano-$CuCr_2O_4$/ultrafine AP composites measured by SEM are presented in Figure 3. As shown in Figure 3a,b, the particle size of ultrafine AP and nano-$CuCr_2O_4$ is 1−5 μm, respectively. In Figure 3c, the particle size of ultrafine AP is consistent with that in Figure 3a before compounding. The particles present a spherical shape, and the surface becomes rough from smooth. It is obvious that

https://doi.org/10.1021/acsomega.1c02002
ACS Omega 2021, 6, 16110−16118

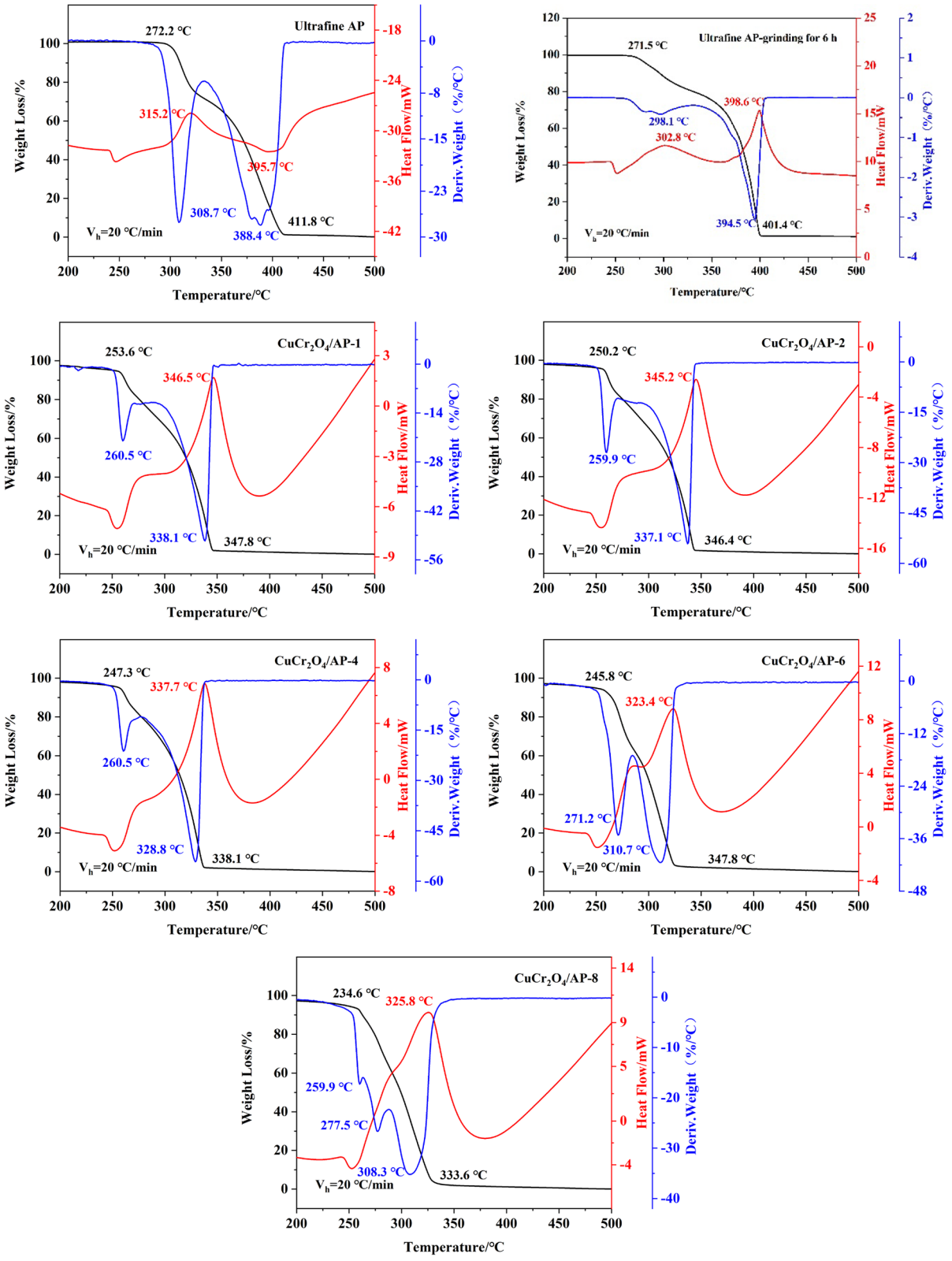

Figure 5. DSC−TG−DTG curves of ultrafine AP, ultrafine AP ground for 6 h, and nano-$CuCr_2O_4$/ultrafine AP composites.

nano-$CuCr_2O_4$ is attached to the surface of ultrafine AP. However, only a small amount of nano-$CuCr_2O_4$ is dispersed on the ultrafine AP, and the dispersion is very uneven. It can be seen from Figure 3d−g that under the force of mechanical ball milling the particle size of some ultrafine AP is further reduced, basically reaching the nanometer level. Moreover, with the increase in the milling time, more and more ultrafine AP particles are further crushed. More and more nano-$CuCr_2O_4$ is dispersed on the surface of ultrafine AP, and its distribution is more uniform. As seen from Figure 3g, the nano-AP gradually accumulates into large spherical particles with a particle size of 5−10 μm. This is mainly due to the long time grinding that

https://doi.org/10.1021/acsomega.1c02002
ACS Omega 2021, 6, 16110−16118

Table 2. Data of Thermal Decomposition Properties of Ultrafine AP and Nano-$CuCr_2O_4$/Ultrafine AP Composites[a]

name of samples	T_e (°C)	T_c (°C)	T_m (°C)	T_L (°C)	T_H (°C)
ultrafine AP	272.2	411.8	388.4	315.2	395.7
$CuCr_2O_4$/AP-1	253.6	347.8	338.1		346.5
$CuCr_2O_4$/AP-2	250.2	346.4	337.1		345.2
$CuCr_2O_4$/AP-3	255.1	345.9	332.7		340.5
$CuCr_2O_4$/AP-4	247.3	338.1	328.8		337.7
$CuCr_2O_4$/AP-5	252.6	324.4	305.3		317.6
$CuCr_2O_4$/AP-6	245.8	347.8	310.7		323.4
$CuCr_2O_4$/AP-7	242.3	340.5	332.2		339.8
$CuCr_2O_4$/AP-8	234.6	333.6	308.3		325.8

[a] T_e is the initial decomposition temperature; T_c is the terminal decomposition temperature; T_m is the maximum weight loss temperature; T_L is the low temperature decomposition temperature; and T_H is the high temperature decomposition temperature.

some water vapor enters into the ball milling tank. The ultrafine AP is very easy to absorb water, so agglomeration occurs. The agglomeration is formed by the stacking of nano-AP, which makes the nano-$CuCr_2O_4$ on the nano-AP enter into the interior of the large spherical AP particles, so the nano-$CuCr_2O_4$ is more evenly dispersed in the ultrafine AP. With the further increase in the ball milling time, the ultrafine AP has no further change. It can be seen from Figure 3 that nano-$CuCr_2O_4$ can be considered to be very evenly dispersed in the ultrafine AP when the ball milling time is 6−12 h.

To better characterize the uniformity of nano-$CuCr_2O_4$/ultrafine AP composites, the surface element distribution characterization of $CuCr_2O_4$/AP-5 is carried out, and the image is shown in Figure 4. It is clear from Figure 4 that in nano-$CuCr_2O_4$/ultrafine AP composite the elements Cu and Cr of nano-$CuCr_2O_4$ are very evenly distributed in the elements Cl, O, and N of ultrafine AP, confirming that the nano-$CuCr_2O_4$ has good dispersion on the surface of ultrafine AP. This shows that nano-$CuCr_2O_4$ can be evenly loaded on the surface of the ultrafine AP via the mechanical grinding method.

3.3. Thermal Analysis. The differential scanning calorimetric (DSC)−thermogravimetric (TG)−thermogravimetric derivative (DTG) curves of ultrafine AP and different nano-$CuCr_2O_4$/ultrafine AP composites at 20 °C/min are shown in Figure 5, and the data of thermal decomposition properties are shown in Table 2. Besides, the DSC−TG−DTG curves of ultrafine AP, which was ground for 6 h, is also shown in Figure 5 for comparison. It can be seen from Figure 5 and Table 2 that after adding nano-$CuCr_2O_4$ the thermal decomposition reaction of the whole ultrafine AP is advanced. From the DSC curve, it can be seen that the low temperature decomposition peak of ultrafine AP is not obvious, and it is basically fused with high temperature decomposition peaks. From the TG curve, it is only a weight loss process. $CuCr_2O_4$/AP-1 and $CuCr_2O_4$/AP-2 prepared by the ultrasonic dispersion and mechanical ball milling methods can reduce the T_H of ultrafine AP from 395.7 to 346.5 and 345.2 °C, respectively, which are decreased by 49.2 and 50.5 °C. It shows that the thermal decomposition performance of nano-$CuCr_2O_4$/ultrafine AP composite prepared by the mechanical ball milling method is better, and the catalytic effect of nano-$CuCr_2O_4$ on ultrafine AP is better. With the increase in the milling time from 0.5 to 48 h, the T_H of ultrafine AP are 345.2, 340.5, 337.7, 317.6, 323.4, 339.8, and 325.8 °C,, which are decreased by 50.5, 55.2, 58.0, 78.1, 72.3, 55.9, and 69.9 °C than those without catalyst, respectively. It is indicated that the catalytic effect of nano-$CuCr_2O_4$ on ultrafine AP increases first and then decreases with the increase in the milling time. It can be seen from the DTG curve that with the increase in the ball milling time, the law of T_m of ultrafine AP is consistent with that of T_H, which further confirms that the catalytic effect of nano-$CuCr_2O_4$ on ultrafine AP first increases and then decreases with the increase in the ball milling time. This is mainly because with the increase in the ball milling time, nano-$CuCr_2O_4$ disperses more evenly in ultrafine AP, showing better catalytic effect. However, when the ball milling time is too long, the catalytic effect of nano-$CuCr_2O_4$ is weakened due to the agglomeration effect. Therefore, the T_H of ultrafine AP is the lowest when the milling time is 6−12 h. It is indicated that the dispersion of nano-$CuCr_2O_4$ in ultrafine AP is the best and the most uniform, so it shows the best catalytic effect.

According to Figure 5, after the ultrafine AP with an average particle size of 1−5 μm was ground for 6 h, its pyrolysis peak temperature changed from 395.7 to 398.6 °C, confirming that the decrease in the high temperature decomposition temperature of the nano-$CuCr_2O_4$/ultrafine AP composite is mainly due to the effect of nano-$CuCr_2O_4$.

The catalytic mechanism of nano-$CuCr_2O_4$ for ultrafine AP is mainly because $CuCr_2O_4$ is a p-type semiconductor with conductive holes, which shows high activity in the oxidation atmosphere and can participate in the electron transfer. The addition of $CuCr_2O_4$ to AP can accelerate the thermal

Table 3. The Comparison of Catalytic Effect of Different on AP Reported in the Literatures and This Study

number	type of catalysts	preparation method of AP composite	usage amount of catalyst (%)	heating rate (°C/min)	T_H (°C)	references
1	$CuCr_2O_4$	mechanical grinding	3	10	305.4	this study
2	$CuCr_2O_4$	mechanical grinding	3	20	317.6	this study
3	$CuCr_2O_4$	thermal decomposition	3	10	331.1	13
4	$CuCr_2O_4$	sol−gel	5	10	338.6	14
5	$CuCr_2O_4$	electrochemical	2	10	349.4	22
6	$CuCr_2O_4$	chemical liquid deposition	6	10	346.0	15
7	CuO	coprecipitation	1	10	350.4	23
8	CuO	surfactant-mediated method	1	10	317.2	24
9	CuO	sol−gel	3	20	353.1	25
10	CuO	hydrothermal	2	20	339.3	26
11	CuO@Cr_2O_3	mechanical grind method	2	20	351.1	27
12	CuO/Fe_2O_3	solid phase method	2	20	335.3	28
13	CNTs/CuO	coprecipitation	8	20	333.1	29

https://doi.org/10.1021/acsomega.1c02002
ACS Omega 2021, 6, 16110−16118

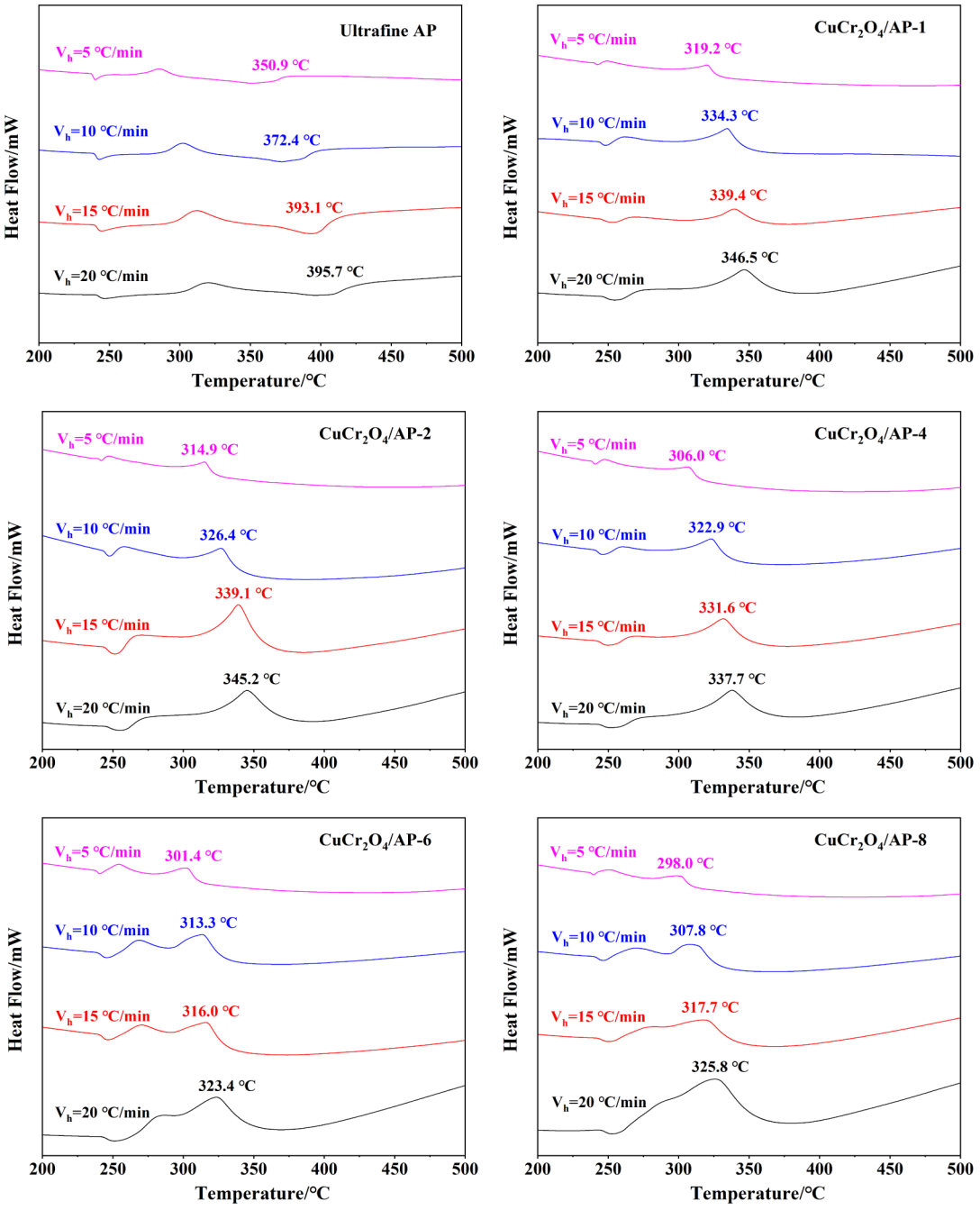

Figure 6. DSC curves of ultrafine AP and nano-$CuCr_2O_4$/ultrafine AP composites at heating rates of 5, 10, 15, and 20 °C/min.

decomposition of AP by a redox reaction with the high temperature decomposition products of AP. After nano-$CuCr_2O_4$ is compounded with ultrafine AP by the mechanical ball milling, the dispersion of nano-$CuCr_2O_4$ in ultrafine AP is more uniform, and the contact area between nano-$CuCr_2O_4$ and ultrafine AP is larger. This is more conducive to the reaction of holes in nano-$CuCr_2O_4$ and oxides decomposed by ultrafine AP at high temperature, thus showing better catalytic performance for ultrafine AP.

The catalytic effect of different catalysts on AP reported in the literatures is listed in Table 3. Compared with other catalysts, T_H of AP decreases to the lowest when $CuCr_2O_4$ is added to AP, which indicates that $CuCr_2O_4$ shows better catalytic effect on AP than most other catalysts. Compared with the reports in other literatures, the prepared nano-$CuCr_2O_4$/ultrafine AP composite in this paper has a lower T_H and better thermal decomposition performance. This is mainly due to the fact that nano-$CuCr_2O_4$ can be more evenly distributed on the ultrafine AP surface by the mechanical grinding method, so it can show better catalytic effect.

3.4. Kinetic Analysis. To further study the pyrolysis of nano-$CuCr_2O_4$/ultrafine AP composites, the thermal decomposition kinetic parameters are calculated. The DSC curves of ultrafine AP and different nano-$CuCr_2O_4$/ultrafine AP composites at heating rates of 5, 10, 15, and 20 °C/min are shown in Figure 6. It can be seen from Figure 6 that with the increase in the heating rate, T_H of nano-$CuCr_2O_4$/ultrafine AP composites gradually increases. This may be due to the fact that with an increase in the heating rate, the heat transfer rate inside the specimen is less than the growth rate of the program

https://doi.org/10.1021/acsomega.1c02002
ACS Omega 2021, 6, 16110−16118

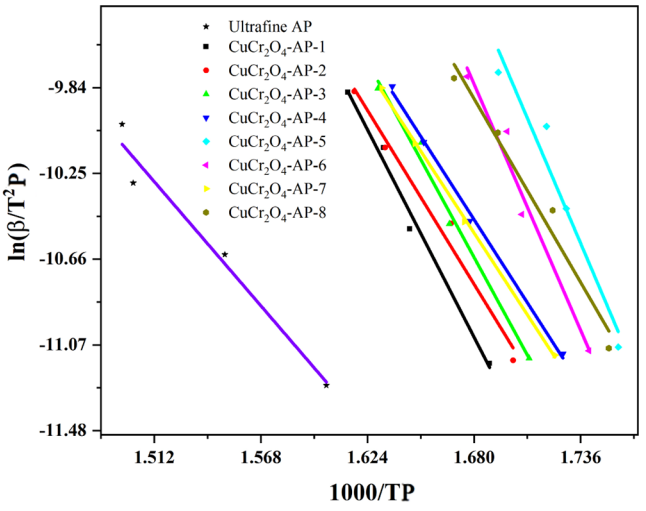

Figure 7. The $\ln(\beta/T_P^2) \sim 1000/T_P$ diagram of ultrafine AP and nano-$CuCr_2O_4$/ultrafine AP composites.

Table 4. Linear Fitting Equations of $\ln(\beta/T_P^2) \sim 1000/T_P$ of Ultrafine AP and Different Nano-$CuCr_2O_4$/Ultrafine AP Composites

name of samples	linear fitting equations	R^2
ultrafine AP	$y = -10.59712x + 5.73371$	0.96955
$CuCr_2O_4$/AP-1	$y = -17.71734x + 18.73228$	0.98826
$CuCr_2O_4$/AP-2	$y = -14.85011x + 14.16850$	0.98123
$CuCr_2O_4$/AP-3	$y = -16.19638x + 17.40815$	0.98723
$CuCr_2O_4$/AP-4	$y = -14.19638x + 13.37943$	0.99703
$CuCr_2O_4$/AP-5	$y = -21.38111x + 26.53310$	0.95128
$CuCr_2O_4$/AP-6	$y = -21.02202x + 25.49423$	0.96962
$CuCr_2O_4$/AP-7	$y = -13.97709x + 12.94707$	0.99923
$CuCr_2O_4$/AP-8	$y = -15.6849x + 16.45807$	0.97340

temperature. Then, the decomposition rate is not able to keep up with the growth rate of the program temperature. This is so-called "temperature hysteresis phenomenon".

For T_H at different heating rates, the Kissinger method is used to calculate the thermal decomposition kinetic parameters of nano-$CuCr_2O_4$/ultrafine AP composites. Figure 7 shows $\ln(\beta/T_P^2) \sim 1000/T_P$ diagram of nano-$CuCr_2O_4$/ultrafine AP composites. Table 4 shows the linear fitting equations of $\ln(\beta/T_P^2) \sim 1000/T_P$ of ultrafine AP and different nano-$CuCr_2O_4$/ultrafine AP composites.

According to the intercept and slope in the linear fitting equation, the thermal decomposition kinetics/kinetic parameters of nano-$CuCr_2O_4$/ultrafine AP composites can be obtained by thermal decomposition calculation, as shown in Table 5.

Table 6. The Impact Sensitivity Data of Ultrafine AP and Nano-$CuCr_2O_4$/Ultrafine AP Composites

name of samples	impact sensitivity H_{50} (cm)	$S_{dev.}$
ultrafine AP	35.1	0.14
$CuCr_2O_4$/AP-1	35.5	0.11
$CuCr_2O_4$/AP-2	35.8	0.12
$CuCr_2O_4$/AP-3	36.9	0.10
$CuCr_2O_4$/AP-4	36.2	0.09
$CuCr_2O_4$/AP-5	37.6	0.09
$CuCr_2O_4$/AP-6	37.1	0.08
$CuCr_2O_4$/AP-7	36.8	0.10
$CuCr_2O_4$/AP-8	37.3	0.11

It can be seen from Table 5 that E_a of high temperature decomposition of nano-$CuCr_2O_4$/ultrafine AP composites prepared by the mechanical ball milling method is lower than that prepared by the ultrasonic dispersion method. With the increase in the milling time, the change in E_a is not obvious. E_a is the lowest when milling for 3 h and then increases significantly at 6−12 h. But with the further milling, it continues to decrease. However, by comparing the $\Delta G^{\neq}$ of nano-$CuCr_2O_4$/ultrafine AP composites, it can be seen that the $\Delta G^{\neq}$ of ultrafine AP decreases significantly after adding nano-$CuCr_2O_4$ catalyst, which indicates that nano-$CuCr_2O_4$ can make the thermal decomposition reaction of ultrafine AP easier. The lowest $\Delta G^{\neq}$ is 142.27 kJ/mol, which is 25.16 kJ/mol lower than that of ultrafine AP, when milling for 6−12 h. It is indicated that nano-$CuCr_2O_4$ has the best catalytic effect in ultrafine AP by the mechanical ball milling for 6−12 h. In the continuous pyrolysis process of AP, nano-$CuCr_2O_4$ accelerates the thermal decomposition of AP and plays the role of adsorption and catalysis. However, nano-$CuCr_2O_4$ is a kind of inorganic substance, which does not contain energy. At this time, there is no continuous heating, which is mainly reflected in the reduction of impact sensitivity. The same results have been reported in many literatures. We have also obtained the similar conclusion that nano-$Cu(OH)_2$ could reduce the sensitivity of AP.[30] In this paper, the activation energy increased, and the A has also increased at the same time, resulting in an increase in the reaction rate k, which reflected in the lower $\Delta G^{\neq}$ value. In this case, the increase in the A (the positive effect on the reaction rate) exceeds the increase in the activation energy (the negative effect on the reaction rate), which is comprehensively reflected by the increase in the reaction rate.[31]

Table 5. The Thermal Decomposition Kinetics/Kinetic Parameters of Ultrafine AP and Nano-$CuCr_2O_4$/Ultrafine AP Composites

name of samples	E_a (kJ/mol)	Ln A (s^{-1})	$k(T_P)$ (s^{-1})	$\Delta S^{\neq}$ (J/mol K)	$\Delta H^{\neq}$ (kJ/mol)	$\Delta G^{\neq}$ (kJ/mol)
ultrafine AP	88.10	15.00	4.30×10^{-1}	−126.92	82.54	167.43
$CuCr_2O_4$/AP-1	147.30	28.51	6.22×10^{-1}	−13.85	142.22	150.68
$CuCr_2O_4$/AP-2	123.46	23.77	5.69×10^{-1}	−53.24	118.39	150.88
$CuCr_2O_4$/AP-3	138.86	27.13	6.54×10^{-1}	−25.25	133.82	149.12
$CuCr_2O_4$/AP-4	118.03	22.94	5.25×10^{-1}	−60.03	113.03	149.16
$CuCr_2O_4$/AP-5	177.76	36.50	6.30×10^{-1}	−53.04	172.95	142.27
$CuCr_2O_4$/AP-6	174.78	35.45	5.73×10^{-1}	−44.23	169.93	144.10
$CuCr_2O_4$/AP-7	116.21	22.49	5.49×10^{-1}	−63.82	111.18	149.81
$CuCr_2O_4$/AP-8	130.40	26.12	4.25×10^{-1}	−33.30	125.57	144.93

https://doi.org/10.1021/acsomega.1c02002
ACS Omega 2021, 6, 16110−16118

3.5. Sensitivity Analysis. The impact sensitivity data of ultrafine AP and nano-$CuCr_2O_4$/ultrafine AP composites are shown in Table 6. It can be seen from Table 6 that the impact sensitivity of nano-$CuCr_2O_4$ combined with ultrafine AP is slightly lower than that of ultrafine AP, and the impact sensitivity tends to decrease with the increase in the ball milling time. This is because nano-$CuCr_2O_4$ coated on the surface of ultrafine AP can absorb and buffer energy, thus reducing the probability of hot spot formation on the surface of ultrafine AP, the impact sensitivity is reduced. As the dispersion of nano-$CuCr_2O_4$ on the surface of ultrafine AP gets better and better, it can play a better role in reducing the sensitivity, and the effect is the best when milling for 6−12 h.

4. CONCLUSIONS

(1) Nano-$CuCr_2O_4$/ultrafine AP composites are successfully prepared by the ultrasonic dispersion and mechanical ball milling methods. Compared with nano-$CuCr_2O_4$/ultrafine AP composite prepared by ultrasonic method, the nano-$CuCr_2O_4$ in ultrafine AP composites prepared by the mechanical ball milling has better dispersion on the ultrafine AP. With the increase in the milling time, the dispersion of nano-$CuCr_2O_4$ on ultrafine AP becomes better and better. When milling for 6−12 h, nano-$CuCr_2O_4$ disperses most evenly in ultrafine AP.

(2) After adding nano-$CuCr_2O_4$, the thermal decomposition performance of ultrafine AP is obviously improved, which shows that the high temperature decomposition temperature is advanced and the Gibbs free energy is reduced. The high temperature decomposition temperature and Gibbs free energy of nano-$CuCr_2O_4$/ultrafine AP composite prepared by ball milling for 6−12 h are the lowest, which decrease at 78.1 °C and 25.16 kJ/mol, respectively, indicating that nano-$CuCr_2O_4$ has the best catalytic effect on ultrafine AP. Moreover, the mechanical sensitivity of nano-$CuCr_2O_4$/ultrafine AP composites is lower than that of ultrafine AP.

AUTHOR INFORMATION

Corresponding Authors

Lei Xiao − *National Special Superfine Powder Engineering Research Center of China, School of Chemical Engineering, Nanjing University of Science and Technology, Nanjing 210094, China;* orcid.org/0000-0001-6716-0066; Email: 15005161138@163.com

Guangpu Zhang − *National Special Superfine Powder Engineering Research Center of China, School of Chemical Engineering, Nanjing University of Science and Technology, Nanjing 210094, China*; Email: gpzhang@njust.edu.cn

Authors

Dongdong Zhang − *National Special Superfine Powder Engineering Research Center of China, School of Chemical Engineering, Nanjing University of Science and Technology, Nanjing 210094, China*

Qiang Li − *Shanxi North Xing'an Chemical Industry Co., Ltd., Taiyuan 030008, China*

Ruiqin Li − *Shanxi North Xing'an Chemical Industry Co., Ltd., Taiyuan 030008, China*

Hao Li − *National Special Superfine Powder Engineering Research Center of China, School of Chemical Engineering, Nanjing University of Science and Technology, Nanjing 210094, China*

Hongxu Gao − *Science and Technology on Combustion and Explosion Laboratory, Xi'an Modern Chemistry Research Institute, Xi'an 710065, China*

Fengqi Zhao − *Science and Technology on Combustion and Explosion Laboratory, Xi'an Modern Chemistry Research Institute, Xi'an 710065, China*

Gazi Hao − *National Special Superfine Powder Engineering Research Center of China, School of Chemical Engineering, Nanjing University of Science and Technology, Nanjing 210094, China*

Wei Jiang − *National Special Superfine Powder Engineering Research Center of China, School of Chemical Engineering, Nanjing University of Science and Technology, Nanjing 210094, China;* orcid.org/0000-0001-5663-9119

Complete contact information is available at: https://pubs.acs.org/10.1021/acsomega.1c02002

Notes

The authors declare no competing financial interest.

ACKNOWLEDGMENTS

This work was financially supported by the Natural Science Foundation of China (Project no. 21805139), China Postdoctoral Science Foundation (no. 2020M673527), and the Fundamental Research Funds for the Central Universities (no. 30919011271).

REFERENCES

(1) Zhang, L. K.; Tian, R. Y.; Zhang, Z. W. Burning rate of AP/HTPB base-bleed composite propellant under free ambient pressure. *Aerosp. Sci. Technol.* **2017**, *62*, 31−35.

(2) Manash, A.; Kumar, P. Comparison of burn rate and thermal decomposition of AP as oxidizer and PVC and HTPB as fuel binder based composite solid propellants. *Def. Technol.* **2019**, *15*, 227−232.

(3) Wang, J. H.; Zhang, W. C.; Zheng, Z. L.; Gao, Y.; Ma, K. F.; Ye, J. H.; Yang, Y. Enhanced thermal decomposition properties of ammonium perchlorate through addition of 3DOM core−shell Fe_2O_3/Co_3O_4 composite. *J. Alloys Compd.* **2017**, *724*, 720−727.

(4) Hedman, T. D.; Gross, M. L. On the thermal stability of partially decomposed ammonium perchlorate. *Propellants, Explos., Pyrotech.* **2016**, *41*, 254−259.

(5) Nagendra, K.; Vijay, C.; Ingole, M.; Ramakrishna, P. A. Combustion of ammonium perchlorate monopropellant: Role of heat loss. *Combust. Flame* **2019**, *209*, 363−375.

(6) Xiao, X. C.; Zhang, Z. Y.; Cai, L. F.; Li, Y. T.; Yan, Z. Y.; Wang, Y. D. The excellent catalytic activity for thermal decomposition of ammonium perchlorate using porous $CuCo_2O_4$ synthesized by template-free solution combustion method. *J. Alloys Compd.* **2019**, *797*, 548−557.

(7) Chaturvedi, S.; Dave, P. N. A review on the use of nanometals as catalysts for the thermal decomposition of ammonium perchlorate. *J. Saudi Chem. Soc.* **2013**, *17*, 135−149.

(8) Vara, J. A.; Dave, P. N.; Chaturvedi, S. The catalytic activity of transition metal oxide nanoparticles on thermal decomposition of ammonium perchlorate. *Def. Technol.* **2019**, *15*, 629−635.

(9) Hu, Y. H.; Tao, B. W.; Shang, F.; Zhou, M. X.; Hao, D. Y.; Fan, R. Q.; Xia, D. B.; Yang, Y. L.; Pan, A. M.; Lin, K. F. Thermal decomposition of ammonium perchlorate over perovskite catalysts: Catalytic decomposition behavior, mechanism and application. *Appl. Surf. Sci.* **2020**, *513*, No. 145849.

(10) Ye, P.; Lu, Y. W.; Xu, P. F.; Hu, X.; He, J. X.; Wang, Q.; Guo, C. P. Preparation of $CoFe_2O_4$@C nano-composites and their catalytic performance for the thermal decomposition of ammonium perchlorate. *Chin. J. Explos. Propell.* **2019**, *42*, 358−362.

(11) Ma, Z. Y.; Li, C.; Wu, R. J.; Chen, R. Z.; Gu, Z. G. Preparation and characterization of superfine ammonium perchlorate (AP)

crystals through ceramic membrane anti-solvent crystallization. *J. Cryst. Growth* **2009**, *311*, 4575−4580.
(12) Dolgoborodov, A. Y.; Streletskii, A. N.; Shevchenko, A. A.; Vorobieva, G. A.; Val'yano, G. E. Thermal decomposition of mechanoactivated ammonium perchlorate. *Thermochim. Acta* **2018**, *669*, 60−65.
(13) Sanoop, A. P.; Rajeev, R.; George, B. K. Synthesis and characterization of a novel copper chromite catalyst for the thermal decomposition of ammonium perchlorate. *Thermochim. Acta* **2015**, *606*, 34−40.
(14) Hosseini, S. G.; Abazari, R.; Gavi, A. Pure $CuCr_2O_4$ nanoparticles: Synthesis, characterization and their morphological and size effects on the catalytic thermal decomposition of ammonium perchlorate. *Solid State Sci.* **2014**, *37*, 72−79.
(15) Eslami, A.; Juibari, N. M.; Hosseini, S. G. Fabrication of ammonium perchlorate/copper-chromium oxides core-shell nanocomposites for catalytic thermal decomposition of ammonium perchlorate. *Mater. Chem. Phys.* **2016**, *181*, 12−20.
(16) Lu, Y. W.; Zhu, Y. F.; Xu, P. F.; Ye, P.; Gao, B.; Sun, Y.; Guo, C. P. In situ synthesis of cobalt alginate/ammonium perchlorate composite and its low temperature decomposition performance. *J. Solid State Chem.* **2018**, *258*, 718−721.
(17) Zhou, Z. X.; Tian, S. Q.; Zeng, D. W.; Tang, G.; Xie, C. S. MOX (M = Zn, Co, Fe)/AP shell−core nanocomposites for self-catalytical decomposition of ammonium perchlorate. *J. Alloys Compd.* **2012**, *513*, 213−219.
(18) Blaine, R. L.; Kissinger, H. E. Homer Kissinger and the Kissinger equation. *Thermochim. Acta* **2012**, *540*, 1−6.
(19) Ge, Z.; Li, X.; Zhang, W.; Sun, Q.; Chai, C.; Luo, Y. Preparation and characterization of ultrafine Fe-O compound/ammonium perchlorate nanocomposites via in-suit growth method. *J. Solid State Chem.* **2018**, *258*, 138−145.
(20) Durrani, S. K.; Hussain, S. Z.; Saeed, K.; Khan, Y.; Ahmed, N. Hydrothermal synthesis and characterization of nanosized transition metal chromite spinels. *Truk. J. Chem.* **2012**, *36*, 111−120.
(21) Appalakutti, S.; Sonawane, S.; Bhanvase, B. A.; Mittal, V.; Ashokkumar, M. Process intensification of copper chromite ($CuCr_2O_4$) nanoparticle production using continuous flow microreactor. *Chem. Eng. Process* **2015**, *89*, 28−34.
(22) Patil, P. R.; Krishnamurthy, V. N.; Joshi, S. S. Effect of nano-copper oxide and copper chromite on the thermal decomposition of ammonium perchlorate. *Propellants, Explos., Pyrotech.* **2008**, *33*, 266−270.
(23) Singh, G.; Kapoor, I. P. S.; Dubey, S.; Siril, P. F. Preparation, characterization and catalytic activity of transition metal oxide nanocrystals. *J. Sci. Conf. Proc.* **2009**, *1*, 11−17.
(24) Fujimura, K.; Miyake, A. The effect of specific surface area of TiO_2 on the thermal decomposition of ammonium perchlorate. *J. Therm. Anal. Calorim.* **2010**, *99*, 27−31.
(25) Alizadeh, G. E.; Shaabani, B.; Khodayari, A.; Azizian-Kalandaragh, Y.; Rahimi, R. Investigation of the catalytic activity of nano-sized CuO, Co_3O_4 and $CuCo_2O_4$ powders on thermal decomposition of ammonium perchlorate. *Powder Technol.* **2012**, *217*, 330−339.
(26) Chen, L. J.; Li, L. P.; Li, G. S. Synthesis of CuO nanorods and their catalytic activity in the thermal decomposition of ammonium perchlorate. *J. Alloys Compd.* **2008**, *464*, 532−536.
(27) Hao, G. Z.; Li, L.; Gou, B. W. Preparation of nano-Cu-Cr composite metal oxides via mechanical grinding method and its catalytic performance for the thermal decomposition of ammonium perchlorate. *Chin. J. Explos. Propell.* **2019**, *42*, 557−565.
(28) Wang, Y. P.; Xia, X. Y.; Zhu, J. W.; Li, Y.; Wang, X.; Hu, X. D. Catalytic activity of nanometer-sized CuO/Fe_2O_3 on thermal decomposition of AP and combustion of AP-based propellant. *Combust. Sci. Technol.* **2010**, *183*, 154−162.
(29) Cui, P.; Wang, A. J. Synthesis of CNTs/CuO and its catalytic performance on the thermal decomposition of ammonium perchlorate. *J. Saudi Chem. Soc.* **2016**, *20*, 343−348.
(30) Hao, G. Z.; Liu, J.; Liu, Q. E.; Xiao, L.; Ke, X.; Gao, H.; Du, P.; Jiang, W.; Zhao, F.; Gao, H. Facile preparation of $AP/Cu(OH)_2$ core-shell nanocomposites and its thermal decomposition behavior. *Propellants, Explos., Pyrotech.* **2017**, *42*, 947−952.
(31) Dhupe, A. P.; Gokarn, A. N.; Doraiswamy, L. K. Investigations into the compensation effect at catalytic gasification of active charcoal by carbon dioxide. *Fuel* **1991**, *70*, 839−844.

https://doi.org/10.1021/acsomega.1c02002
ACS Omega 2021, 6, 16110−16118